Strongly correlated electrons

M. Angst

This document has been published in

Thomas Brückel, Gernot Heger, Dieter Richter, Georg Roth and Reiner Zorn (Eds.):
Lectures of the JCNS Laboratory Course held at Forschungszentrum Jülich and the research reactor FRM II of TU Munich
In cooperation with RWTH Aachen and University of Münster
Schriften des Forschungszentrums Jülich / Reihe Schlüsseltechnologien / Key Technologies, Vol. 39
JCNS, RWTH Aachen, University of Münster
Forschungszentrum Jülich GmbH, 52425 Jülich, Germany, 2012
ISBN: 978-3-89336-789-4

12 Strongly correlated electrons

M. Angst
Peter Grünberg Institut 4
Forschungszentrum Jülich GmbH

Contents

Lecture Notes of the JCNS Laboratory Course Neutron Scattering

12.1 Introduction

Materials with strong electronic correlations are materials, in which the movement of one electron depends on the positions and movements of all other electrons due to the long-range Coulomb interaction. With this definition, one would naively think that all materials show strong electronic correlations. However, in purely ionic systems, the electrons are confined to the immediate neighborhood of the respective atomic nucleus. On the other hand, in ideal metallic systems, the other conduction electrons screen the long-range Coulomb interaction. Therefore, while electronic correlations are also present in these systems and lead for example to magnetism, the main properties of the systems can be explained in simple models, where electronic correlations are either entirely neglected (e.g. the free electron Fermi gas) or taken into account only in low order approximations (Fermi liquid, exchange interactions in magnetism etc.). In highly correlated electron systems, simple approximations break down and entirely new phenomena and functionalities can appear. These so-called *emergent* phenomena cannot be anticipated from the local interactions among the electrons and between the electrons and the lattice [1]. This is a typical example of *complexity*: the laws that describe the behavior of a complex system are qualitatively different from those that govern its units [2]. This is what makes highly correlated electron systems a research field at the very forefront of condensed matter research. The current challenge in condensed matter physics is that we cannot reliably predict the properties of these materials. There is no theory, which can handle this huge number of interacting degrees of freedom. While the underlying fundamental principles of quantum mechanics (Schrödinger equation or relativistic Dirac equation) and statistical mechanics (maximization of entropy) are well known, there is no way at present to solve the many-body problem for some 10^{23} particles. Some of the exotic properties of strongly correlated electron systems and examples of emergent phenomena and novel functionalities are:

- *High temperature superconductivity*; while this phenomenon was discovered in 1986 by Bednorz and Müller [3], who received the Nobel Prize for this discovery, and since then has continually attracted the attention of a large number of researchers, there is still no commonly accepted mechanism for the coupling of electrons into Cooper pairs, let alone a theory which can predict high temperature superconductivity or its transition temperatures. High temperature superconductivity has already some applications such as highly sensitive magnetic field sensors, high field magnets, and power lines, and more are likely in the future.

- *Colossal magnetoresistance* effect CMR, which was discovered in transition metal oxide manganites and describes a large change of the electrical resistance in an applied magnetic field [4]. This effect can be used in magnetic field sensors and could eventually replace the giant magnetoresistance [5, 6] field sensors, which are employed for example in the read heads of magnetic hard discs.

- The *magnetocaloric* effect [7], a temperature change of a material upon applying a magnetic field, can be used for magnetic refrigeration without moving parts or cooling fluids.

- *Metal-insulator-transitions* as observed e.g. in magnetite (Verwey transition [8]) or certain vanadites are due to strong electronic correlations and could be employed as electronic switches.

- *Multiferroicity* [9], the simultaneous occurring of various ferroic orders, e.g. ferromagnetism and ferroelectricity, in one material. If the respective degrees of freedom are strongly coupled, one can switch one of the orders by applying the conjugate field of the other order. Interesting for potential applications in information technology is particularly the switching of magnetization by an electric field, which has been proposed to be used for easier switching of magnetic non-volatile memories [10]. Future applications of multiferroic materials in computer storage elements are apparent. One could either imagine elements, which store several bits in form of a magnetic- and electric polarization, or one could apply the multiferroic properties for an easier switching of the memory element.
- *Negative thermal expansion* [11] is just another example of the novel and exotic properties that these materials exhibit.

It is likely that many more such emergent phenomena will be discovered in the near future. This huge potential is what makes research on highly correlated electron systems so interesting and challenging: this area of research is located right at the intersection between fundamental science investigations, striving for basic understanding of the electronic correlations, and technological applications, connected to the new functionalities [12].

12.2 Electronic structure of solids

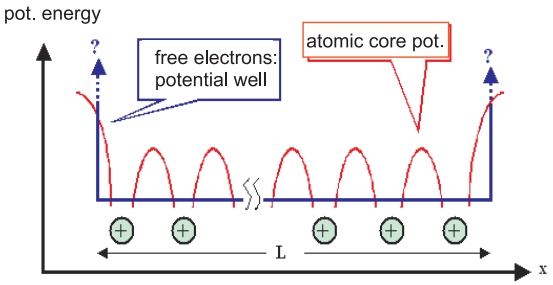

Fig. 12.1: *Potential energy of an electron in a solid.*

In order to be able to discuss the effects of strong electronic correlations, let us first recapitulate the textbook knowledge of the electronic structure of solids [13, 14]. The description of the electron system of solids usually starts with the adiabatic or Born-Oppenheimer approximation: The argument is made that the electrons are moving so quickly compared to the nuclei that the electrons can instantaneously follow the movement of the much heavier nuclei and thus see the instantaneous nuclear potential. This approximation serves to separate the lattice- and electronic degrees of freedom. Often one makes the further approximation to consider the nuclei to be at rest in their equilibrium positions. The potential energy seen by a single electron in the averaged field of all other electrons and the atomic core potential is depicted schematically for a one dimensional system in Fig. 12.1.

The following simple models are used to describe the electrons in a crystalline solid:

- *Free electron Fermi gas*: here a single electron moves in a 3D potential well with infinitely high walls corresponding to the crystal surfaces. All electrons move completely

independent, i.e. the interaction between the electrons is considered only indirectly by the Pauli exclusion principle.

- *Fermi liquid*: here the electron-electron interaction is accounted for in a first approximation by introducing *quasiparticles*, so-called dressed electrons, which have a charge e, and a spin $\frac{1}{2}$ like the free electron, but an effective mass m^*, which can differ from the free electron mass m. Other than this renormalization, interactions are still neglected.

- *Band structure model*: this model takes into account the periodic potential of the atomic cores at rest, i.e. the electron moves in the average potential from the atomic cores and from the other electrons.

Considering the strength of the long-range Coulomb interaction, it is surprising that the simple models of Fermi gas − or better Fermi liquid − already are very successful in describing some basic properties of simple metals. The band structure model is particularly successful to describe semiconductors. But all three models have in common that the electron is described with a single particle wave function and electronic correlations are only taken into account indirectly, to describe phenomena like magnetism due to the exchange interaction between the electrons or BCS superconductivity [15], where an interaction between electrons is mediated through lattice vibrations and leads to Cooper pairs, which undergo a Bose-Einstein condensation.

What we have sketched so far is the textbook knowledge of introductory solid state physics courses. Of course there exist more advanced theoretical descriptions, which try to take into account the electronic correlations. The strong Coulomb interaction between the electrons is taken into account in density functional theory in the so-called "LDA+U" approximation or in so-called dynamical mean field theory DMFT or a combination of the two in various degrees of sophistication [16]. Still, all these extremely powerful and complex theories often fail to predict even the simplest physical properties, such as whether a material is a conductor or an insulator.

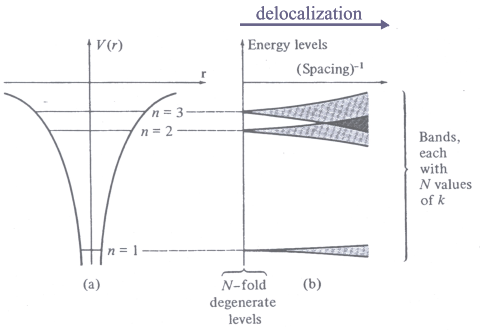

Fig. 12.2: Left*: Atomic potential of an electron interacting with the atomic core and the corresponding level scheme of sharp energy levels.* Right*: Broadening of these levels into bands upon increase of the overlap of the wave functions of neighboring atoms.*

Let us come back to the band structure of solids. In the so-called tight-binding model one starts from isolated atoms, where the energy levels of the electrons in the Coulomb potential of the corresponding nucleus can be calculated. If N such atoms are brought together, the wave functions of the electrons from different sites start to overlap, leading to a broadening of the atomic energy levels, which eventually will give rise to the electronic bands in solids, each of which is a quasi-continuum of N electronic states. The closer the atoms are brought together,

the more the wave functions overlap, the more the electrons will be delocalized, and the broader are the corresponding bands (Fig. 12.2).

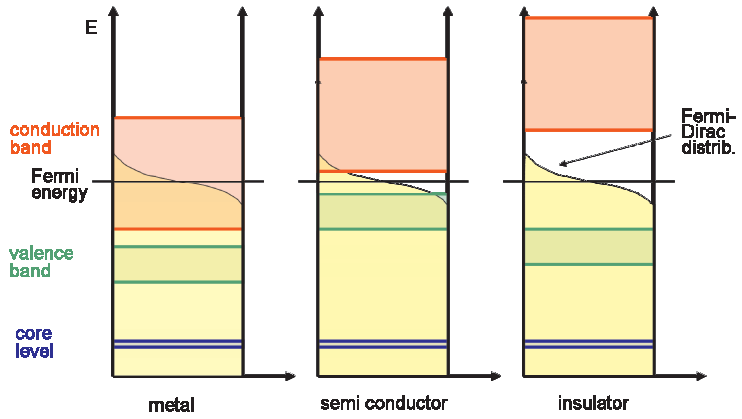

Fig. 12.3: *band structure of metals, semiconductors, and instulators.*

If electronic correlations are not too strong, the electronic properties can be described by a band structure, which allows one to predict whether a material is a metal, a semiconductor or an insulator. This is shown in Fig. 12.3. At $T = 0$ all electronic states are being filled up to the Fermi energy. At finite T the Fermi-Dirac distribution describes the occupancy of the energy levels. If the Fermi energy lies somewhere in the middle of the conduction band, the material will be metallic. If it lies in the middle between valence band and conduction band and these two are separated by a large/small gap (compared to the energy equivalent of room temperature) the material will show insulating/semiconducting behavior. However, as mentioned above this band structure model describes the electrons with single particle wave functions. Where are the electronic correlations?

12.3 Strong electronic correlations: the Mott transition

Fig. 12.4: *Rock-salt (NaCl)-type structure of CoO.*

It turns out that electronic correlations are particularly important in materials, which have some very narrow bands. This occurs for example in transition metal oxides or transition metal chalcogenides as well as in some light rare earth intermetallics (heavy fermion systems). Consider CoO as a typical and simple example of a transition metal oxide. CoO has the rock-salt

structure shown in Fig. 12.4, with a face-centered cubic (fcc) unit cell containing four formula units. The primitive unit cell of the fcc lattice, however, is spanned by the basis vectors

$$\mathbf{a}' = \frac{1}{2}a(\mathbf{e}_x + \mathbf{e}_y); \quad \mathbf{b}' = \frac{1}{2}a(\mathbf{e}_y + \mathbf{e}_z); \quad \mathbf{c}' = \frac{1}{2}a(\mathbf{e}_z + \mathbf{e}_x). \tag{12.1}$$

Here, a is the lattice constant, and $\mathbf{e}_x$, $\mathbf{e}_y$, and $\mathbf{e}_y$, are the unit basis vectors of the original fcc unit cell. Therefore the primitive unit cell contains exactly one cobalt and one oxygen atom. The electronic configurations of these atoms are: Co: [Ar]$3d^7 4s^2$; O: [He]$2s^2 2p^4$. In the solid, the atomic cores of Co and O have the electronic configuration of Ar and He, respectively. These electrons are very strongly bound to the nucleus and we need not consider them on the usual energy scales for excitations in the solid state. We are left with nine outer electrons for the Co and six outer electrons for the O atom in the solid, so that the total number of electrons per primitive unit cell is $9 + 6 = 15$, i.e. an odd number. According to the Pauli principle, each electronic state can be occupied by two electrons, one with spin up and one with spin down. Therefore with an odd number of electrons, we must have at least one partially filled band and according to Fig. 12.1, CoO must be a metal.

What does experiment tell us? Well, in fact, CoO is a very good insulator with a room-temperature resistivity $\rho(300\,\mathrm{K}) \sim 10^8\,\Omega\mathrm{cm}$ (For comparison, the good conductor iron has $\rho(300\,\mathrm{K}) \sim 10^{-7}\,\Omega\mathrm{cm}$. The resistivity of CoO corresponds to activation energies of about $0.6\,\mathrm{eV}$ or a temperature equivalent of $7000\,\mathrm{K}$, which means there is a huge band gap making CoO a very good insulator. To summarize these considerations: the band theory breaks down already for a very simple oxide consisting of only one transition metal and one oxygen atom!

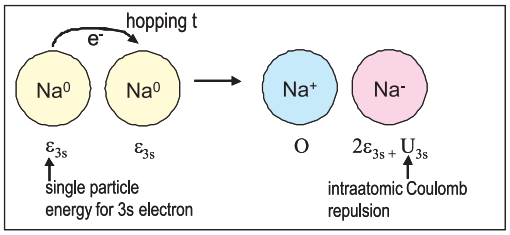

Fig. 12.5: *Illustration of (electron) hopping between two neutral Na atoms - involving charge fluctuations.*

In order to understand the reason for this dramatic breakdown of band theory, let us consider an even simpler example: the alkali metal sodium (Na) with the electronic configuration [Ne]$3s^1$=$1s^2 2s^2 2p^6 3s^1$. Following our argumentation for CoO, sodium obviously has a half-filled 3s band and is therefore a metal. This time our prediction was correct: $\rho(300\,\mathrm{K}) \sim 5 \times 10^{-6}\,\Omega\mathrm{cm}$. However, what happens if we pull the atoms further apart and increase the lattice constant continuously? Band theory predicts that for all distances sodium remains a metal, since the 3s band will always be half-filled. This contradicts our intuition and of course also the experiment: at a certain critical separation of the sodium atoms, there must be a transition from a metal to an insulator. This metal-to-insulator transition was predicted by Sir Nevill Mott (physics Nobel price 1977), which is therefore called the Mott-transition [17]. The physical principle is illustrated in Fig. 12.5: On the left, two neutral Na atoms are depicted. The atomic energy levels of the outer electrons correspond to an energy ε_{3s}. The wave functions of the 3s electrons will overlap giving rise to a finite probability that an electron can hop from one sodium atom to the other one. Such a delocalization of the electrons arising from their possibility to hop

is favored because it lowers their kinetic energy. This can be seen for example by generalizing the "particle in a box" problem: $E_{\text{kin}} \propto p^2 = h^2/\lambda^2$ (de Broglie) and $\lambda \sim$box dimension, and it is consistent with the uncertainty principle $\Delta p \cdot \Delta x \geq \frac{\hbar}{2}$. Fig. 12.5 on the right shows the situation after the electron transfer. Instead of neutral atoms, we have one Na^+ and one Na^- ion. However, we have to pay a price for the double occupation of the 3s states on the Na^- ion, namely the intra-atomic Coulomb repulsion between the two electrons denoted as U_{3s}. While this is a very simplistic picture, where we assume that the electron is either located on one or the other Na atom, this model describes the two main energy terms by just two parameters: the hopping matrix element t, connected to the kinetic energy, and the intra-atomic Coulomb repulsion U, connected with the potential energy due to the Coulomb interaction between the two electrons on one site. In this simple model, we have replaced the long range Coulomb potential proportional to $1/r$ with its leading term, an on-site Coulomb repulsion U. More realistic models would have to take higher order terms into account but already such a simple consideration leads to very rich physics. We can see from Fig. 12.5 that electronic conductivity is connected with charge fluctuations and that such charge transfer costs energy, where U is typically in the order of 1 or $10\,\text{eV}$. Only if the gain in kinetic energy due to the hopping t is larger than the penalty in potential energy U can we expect metallic behavior. If the sodium atoms are now being separated more and more, the intra-atomic Coulomb repulsion U will maintain its value while the hopping matrix element t, which depends on the overlap of the wave functions, will diminish. At a certain critical value of the lattice parameter a, potential energy will win over kinetic energy and conductivity will be suppressed. This is the physical principle behind the Mott transition.

More formally, this model can be cast into a model Hamiltonian, the so-called Hubbard model [18]. In second quantization of quantum-field theory, the corresponding Hamiltonian is

$$\hat{\mathcal{H}} = -t \sum_{j,l,\sigma} (\hat{c}^\dagger_{j\sigma} \hat{c}_{l\sigma} + \hat{c}^\dagger_{l\sigma} \hat{c}_{j\sigma}) + U \sum_j \hat{n}_{j\uparrow} \hat{n}_{j\downarrow}, \tag{12.2}$$

where the operator $\hat{c}^\dagger_{j\sigma}$ creates an electron in the atomic orbital $\Phi(\mathbf{r} - \mathbf{R}_j)|\sigma\rangle$. The first term is nothing but the tight-binding model of band structure (in second quantization), where t is the hopping amplitude depending on the overlap of the wavefunctions from nearest-neighbor atoms at $\mathbf{R}_1$ and $\mathbf{R}_2$:

$$t = \int \Phi(\mathbf{r} - \mathbf{R}_1) \frac{e^2}{4\pi\varepsilon_0 \left|\mathbf{r} - \mathbf{R}_2\right|} \Phi(\mathbf{r} - \mathbf{R}_2)\, d\mathbf{r}. \tag{12.3}$$

It describes the kinetic energy gain due to electron hopping.

The second term is the potential energy due to doubly-occupied orbitals. Here, $\hat{n}_{j\sigma} = \hat{c}^\dagger_{j\sigma} \hat{c}_{j\sigma}$ is the occupation operator of the orbital $\Phi(\mathbf{r} - \mathbf{R}_j)|\sigma\rangle$ and U is the Coulomb repulsion between two electrons in this orbital,

$$U = \int \frac{e^2 \left|\Phi(\mathbf{r}_1 - \mathbf{R}_j)\right|^2 \left|\Phi(\mathbf{r}_2 - \mathbf{R}_j)\right|^2}{4\pi\varepsilon_0 \left|\mathbf{r}_1 - \mathbf{r}_2\right|}\, d\mathbf{r}_1 d\mathbf{r}_2, \tag{12.4}$$

The Hubbard model is a so-called *lattice fermion model*, since only discrete lattice sites are being considered. It is the simplest way to incorporate correlations due to the Coulomb interaction since it takes into account only the strongest contribution, the on-site Coulomb interaction. Still there is very rich physics contained in this simple Hamiltonian like the physics of ferromagnetic-

or antiferromagnetic metals and insulators, charge- and spin density waves and so on [18]. A realistic Hamiltonian should contain many more inter-site terms due to the long-range Coulomb interaction likely to contain additional new physics.

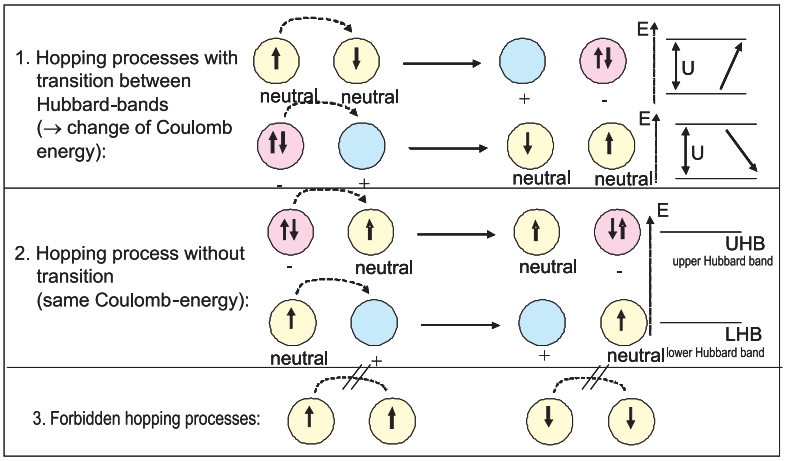

Fig. 12.6: *Illustration of hopping processes between neighboring atoms together with their corresponding energy scales.*

The most direct consequence of the on-site Coulomb interaction is that additional so-called Hubbard bands are created due to possible hopping processes, illustrated in Fig. 12.6: The first row shows hopping processes involving a change of the total Coulomb energy. The second row shows hopping processes without energy change. The last row shows hopping processes forbidden due to the Pauli principle (here, the spin enters the model, giving rise to magnetic order). From Fig. 12.6 we can identify two different energy states. Configurations for which the on-site Coulomb repulsion comes into play have an energy which is higher by the on-site Coulomb repulsion U as compared to such configurations where the electrons are not on the same atom. In a solid these two energy levels will broaden into bands (due to the delocalization of the electrons on many atoms driven by the hopping matrix element t), which are called the lower Hubbard band and the upper Hubbard band. If these bands are well separated, i.e. the Coulomb repulsion U dominates over the hopping term t, we will have in insulating state (only the lower Hubbard band is occupied). If the bands overlap, we will have a metallic state. Note that lower and upper Hubbard band are totally different from the usual band structure of solids as they do not arise due to the interaction of the electrons with the atomic cores but due to electronic correlations. As a result the existence of the Hubbard bands depends on the electronic occupation: the energy terms for simple hopping processes depend on the occupation of neighboring sites. The apparently simple single electron operator gets complex many body aspects.

12.4 Complex ordering phenomena: perovskite manganites as example

The correlation-induced localization leads to atomic-like electronic degrees of freedom that can order in complex ways. In the following we will discuss these ordering processes, taking as an

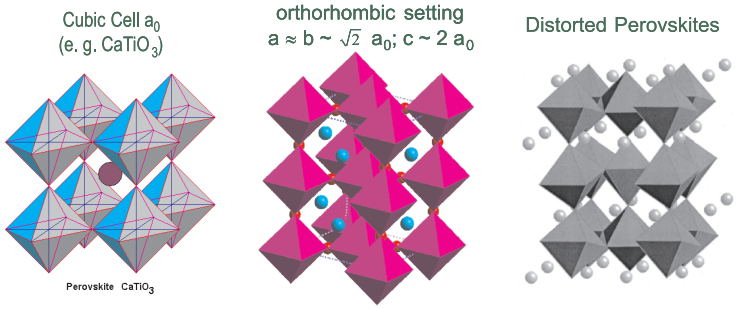

Fig. 12.7: *Perovskite structures. Left: Ideal (cubic) structure. Middle: cubic structure in orhorhombic setting. Right: distorted structure with rotated and tilted oxygen octahedra.*

example perovskite manganites (see e.g. [19]). Their stoichiometric formula is $A_{1-x}B_x\mathrm{MnO_3}$, where A is a trivalent cation (e.g. $A =$ La, Gd, Tb, Er, Y, Bi) and B is a divalent cation ($B =$ Sr, Ca, Ba, Pb). The doping with divalent cations leads to a mixed valence on the manganese sites. In a purely ionic model (neglecting covalency) charge neutrality requires that manganese exists in two valence states: $\mathrm{Mn^{3+}}$ (electronic configuration [Ar]$3d^4$, note that the 5s electrons are lost first upon positive ionization) and $\mathrm{Mn^{4+}}$ ([Ar]$3d^3$) according to the respective doping levels: $A_{1-x}B_x\mathrm{MnO_3} \rightarrow \left[A^{3+}_{1-x}B^{2+}_x\right]\left[\mathrm{Mn}^{3+}_{1-x}\mathrm{Mn}^{4+}_x\right]\mathrm{O}^{2-}_3$. The structure of these mixed valence manganites is related to the perovskite structure (Fig. 12.7). Perovskite $CaTiO_3$ is a mineral, which has a cubic crystal structure, where the smaller $\mathrm{Ca^{2+}}$ metal cation is surrounded by six oxygen atoms forming an octahedron; these corner sharing octahedra are centered on the corners of a simple cubic unit cell and the larger $\mathrm{Ti^{4+}}$ metal cation is filling the interstice in the center of the cube. This ideal cubic perovskite structure is extremely rare. It only occurs when the sizes of the metal ions match to fill the spaces be-tween the oxygen atoms ideally. Usually there is a misfit of the mean ionic radii of the A and B ions, which leads to sizeable tilts of the oxygen octahedra. The resulting structure is related to the perovskite structure as illustrated in Fig. 12.7: in the middle the cubic perovskite structure is shown in a different, orthorhombic setting. The usually observed (e.g. for $LaMnO_3$) perovskite structure is related to this structure by a tilting of the corner shared oxygen octahedra as shown on the right.

For the manganites the octahedral surrounding of the Mn ions leads to so-called crystal field effects. To explain these we stay in the ionic model and describe the oxygen atoms as $\mathrm{O^{2-}}$ ions. The outer electrons of the Mn ions, the 3d electrons, experience the electric field created by the surrounding $\mathrm{O^{2-}}$ ions of the octahedral environment. This leads to a splitting of the electronic levels by the crystal field as depicted in Fig. 12.8: The 3d orbitals with lobes of the electron density pointing towards the negatively charged oxygen ions ($3z^2 - r^2$ and $x^2 - y^2$; so-called e_g orbitals) will have higher energies with respect to the orbitals with the lobes pointing in-between the oxygen atoms (zx, yz, and xy; so-called t_{2g} orbitals). For the manganites this crystal-field splitting is typically $\sim 2\,\mathrm{eV}$. If we now consider a $\mathrm{Mn^{3+}}$ ion, how the electrons will occupy these crystal field levels depends on the ratio between the crystal-field splitting and the intra-atomic exchange: According to the first of Hunds' rules, electrons tend to maximize the total spin, i.e. occupy energy levels in such a way that the spins of all electrons are parallel as far as Pauli principle permits. This is a consequence of the Coulomb interaction within a single atom and is expressed by the Hunds' rule energy J_H. If the crystal field splitting is much larger than Hunds' coupling, a *low-spin state* results, where all electrons are in the lower t_{2g} level and two of these t_{2g} orbitals are singly occupied and one is doubly occupied. Due to the Pauli principle

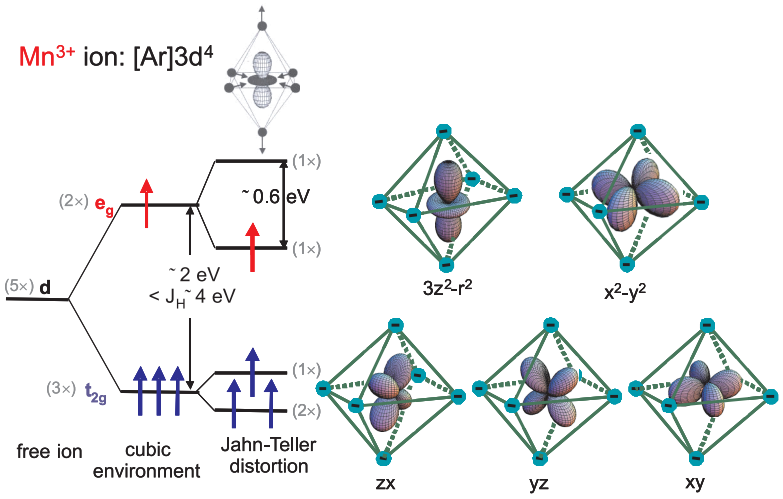

Fig. 12.8: *Energy level diagram for a MnO^{3+} ion in an oxygen octahedron. For the free ion, the four 3d electron levels are degenerate. They split in a cubic environment into t_{2g} and e_g levels. If Hunds' rule coupling is stronger than crystal field splitting, a high spin state results. The degeneracy of the e_g level is lifted by a Jahn-Teller distortion resulting in an elongation of the oxygen octahedra. On the right of the figure, the a basis set of 5* real *3d orbitals are depicted.*

the spins in the doubly occupied orbital have to be antiparallel, giving rise to a total spin $S = 1$ for this low spin state. Usually, however, in the manganites Hunds' rule coupling amounts to $\sim 4\,\mathrm{eV}$, stronger than the crystal field splitting. In this case the *high spin state* shown in Fig. 12.8 is realized, where four electrons with parallel spin occupy the three t_{2g} orbitals plus one of the two e_g orbitals. The high spin state has a total spin of $S = 2$ and the orbital angular momentum is quenched, i.e. $L = 0$. This state has an orbital degree of freedom: the e_g electron can either occupy the $3z^2 - r^2$ or the $x^2 - y^2$ orbital. The overall energy can (and thus will) be lowered by a geometrical distortion of the oxygen octahedra that shifts the e_g levels, lifting their degeneracy This so-called *Jahn-Teller effect* (Fig. 12.8) further splits the d-electron levels. For the case shown, the c-axis of the octahedron has been elongated, thus lowering the energy of the $3z^2 - r^2$ orbital with respect to the energy level of the $x^2 - y^2$ orbital. The Jahn-Teller splitting in the manganites has a magnitude of typically $\sim 0.6\,\mathrm{eV}$.

The Jahn-Teller effect demonstrates nicely how in these transition metal oxides electronic and lattice degrees of freedom are coupled. Only the Mn^{3+} with a single electron in the e_g orbitals exhibits the Jahn-Teller effect, whereas the Mn^{4+} ion does not. A transfer of charge between neighboring manganese ions is accompanied with a change of the local distortion of the oxygen octahedron: a so-called lattice polaron. Due to the Jahn-Teller effect, charge fluctuations and lattice distortions become coupled in these mixed-valence oxides.

Having explained the Jahn-Teller effect, we can now introduce an important type of electronic order occurring in these materials: *orbital order*. Consider the structure of $LaMnO_3$: All manganese are trivalent and are expected to undergo a Jahn-Teller distortion. In order to minimize the elastic energy of the lattice, the Jahn-Teller distortions on neighboring sites are correlated. Below a certain temperature $T_{\mathrm{JT}} \sim 780\,\mathrm{K}$, a cooperative Jahn-Teller transition takes place, with a distinct pattern of distortions of the oxygen octahedra throughout the crystal lattice as shown in Fig. 12.9 left. This corresponds to a long-range orbital order of the e_g electrons, not to be confused with magnetic order of an orbital magnetic moment. In fact, the orbital magnetic mo-

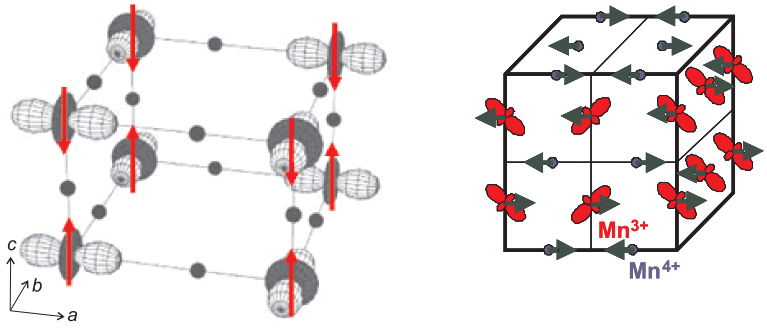

Fig. 12.9: Left*: Orbital order in $LaMnO_3$. Below the Jahn-Teller transition temperature of* $780\,\mathrm{K}$*, a distinct long range ordered pattern of Jahn-Teller distortions of the oxygen octahedra occurs leading to orbital order of the e_g orbitals of the Mn^{3+} ions as shown. Also shown is the antiferromagnetic spin order which sets in below the Néel temperature* $T_\mathrm{N} \sim 145\,\mathrm{K}$*. Oxygen atoms are represented by filled circles, La is not shown.* Right*: Charge-, orbital- and spin-order in half-doped manganite $La^{3+}_{0.5}Sr^{2+}_{0.5}Mn3{+}_{0.5}Mn2{+}_{0.5}O_3$.*

ment is quenched, i.e. totally suppressed, by the crystal field surrounding the Mn^{3+} ions (this is always the case for non-degenerate states with real wave functions because such functions have pure-imaginary expectation values for an angular momentum operator). Orbital ordering instead denotes a long-range ordering of an anisotropic charge distribution around the nuclei. As the temperature is further lowered, magnetic order sets in at $T_\mathrm{N} \sim 145\,\mathrm{K}$. In $LaMnO_3$ the spin degree of freedom of the Mn^{3+} ion orders antiferromagnetically in so-called A-type order: spins within the a-b plane are parallel, while spins along c are coupled antiferromagnetically. This d-type orbital ordering and A-type antiferromagnetic ordering results from a complex interplay between structural-, orbital- and spin degrees of freedom and the relative strengths of the different coupling mechanisms in $LaMnO_3$.

Doped manganites are even more complex, because the charge on the Mn site becomes an additional degree of freedom due to the two possible manganese valances Mn^{3+} and Mn^{4+}. In order to minimizes the Coulomb interaction between neighboring manganese sites, so-called charge order can develop. This is shown for the example of half-doped manganites in Fig. 12.9 on the right: These half-doped manganites show antiferromagnetic spin order, a checkerboard-type charge order with alternating Mn^{3+} and Mn^{4+} sites and a zig-zag orbital order of the additional e_g electron present on the Mn^{3+} sites. This is only one example of the complex ordering phenomena that can occur in doped mixed valence manganites. These ordering phenomena result from a subtle interplay between lattice-, charge-, orbital-, and spin degrees of freedom and can have as a consequence novel phenomena and functionalities such as colossal magnetoresistance.

How are these ordering phenomena related with the macroscopic properties of the system? To answer this question, let us look at the resistivity of doped Lanthanum-Strontium-Manganites (Fig. 12.10): The zero field resistance changes dramatically with composition. The $x = 0$ compound shows insulating behavior: the resistivity ρ increases with decreasing temperature T. The higher doped compounds, e.g. $x = 0.4$, are metallic with $\rho(T)$ decreasing. Note, however, that the resistivity of these compounds is still about three orders of magnitude higher than for typical good metals. At an intermediate composition $x = 0.15$, the samples are insulators at higher T down to about $250\,\mathrm{K}$, then a dramatic drop of the resistivity indicating an insulator-to-metal transition and again an upturn below about $210\,\mathrm{K}$ with typical insulating behavior.

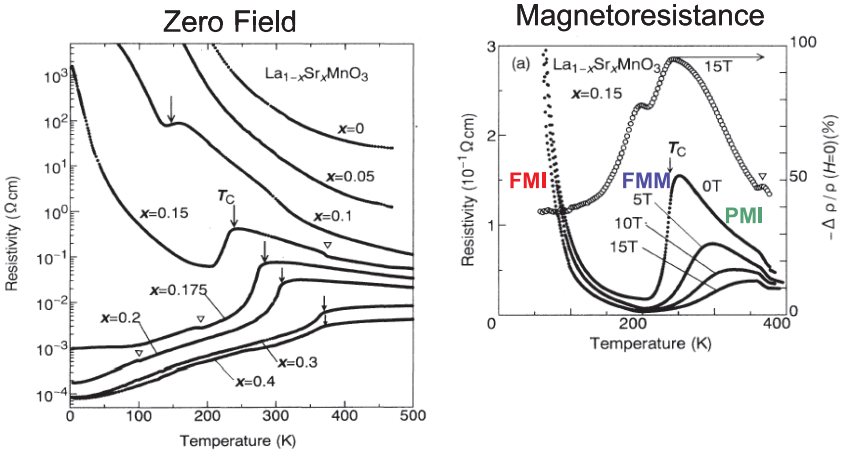

Fig. 12.10: *Resistivity in the $La_{1-x}Sr_xMnO_3$ series [20].* Left*: resistivity in zero field for various compositions from $x = 0$ to $x = 0.5$.* Right*: resistivity for $x = 0.15$ in different magnetic fields H, and magnetoresistance, defined as the change in resistivity relative to its value for $H = 0$.*

The metal-insulator transition occurs at the temperature where ferromagnetic long-range order sets in. Around this temperature we also observe a very strong dependence of resistivity on external magnetic field. This is the so-called *colossal magnetoresistance* effect. In order to appreciate the large shift in the maximum of the resistivity curve with field (Fig. 12.10 right) one should remember that the energy scales connected with the Zeeman interaction of the spin $\frac{1}{2}$ electron in an applied magnetic field are very small: the energy equivalent of 1 Tesla for a spin $\frac{1}{2}$ system corresponds to $0.12\,\mathrm{meV}$, which in turn corresponds to a temperature equivalent of $1.3\,\mathrm{K}$. The strong dependence of the resistance on an external field is partly due to the so-called *double exchange* mechanism: the electron hopping from Mn^{3+} to Mn^{4+} (associated with metallicity) can occur only if the t_{2g} spins are parallel, which is automatically fulfilled (only) in the ferromagnetic state. This phase competition and consequent tunability by external parameters, such as temperature and field, is typical for correlated-electron systems.

It is clear that our entire discussion starting from ionic states is only a crude approximation to the real system. Therefore we now have to pose the question how can we determine the true valence state? Or more general, which experimental methods exist to study the complex ordering and excitations of the charge-, orbital-, spin- and lattice- degrees of freedom in these complex transition metal oxides?

12.5 Probing correlated electrons by scattering methods

How can these various ordering phenomena be studied experimentally? Obviously we need probes with atomic resolution, which interact with the spins as well as with the charges in the system. Therefore neutron and x-ray scattering are the ideal microscopic probes to study the complex ordering phenomena and their excitation spectra. The lattice and spin structure can be studied with neutron diffraction from a polycrystalline or single crystalline sample as detailed in chapter 8 of this course, "Structural analysis". Fig. 12.11 shows as an example a powder spectrum of a $La_{7/8}Sr_{1/8}MnO_3$ material. Neutrons also allow one to determine the magnetic

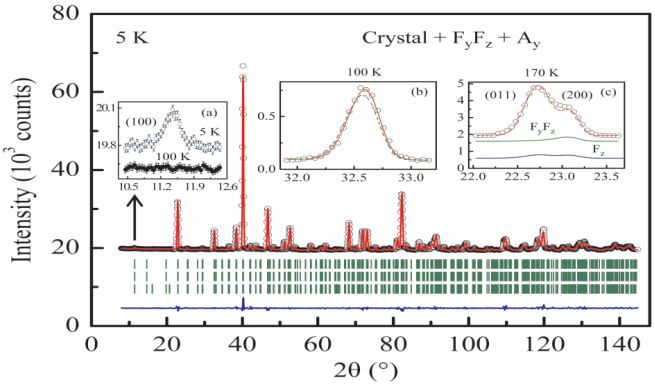

Fig. 12.11: *High resolution neutron powder diffractogram of a powdered single crystal of* $La_{\frac{7}{8}}Sr_{\frac{1}{8}}MnO_3$. ○*: data points, line: structural refinement. Structural and magnetic Bragg reflections are located at the 2 values indicated by the vertical lines below the spectrum. The solid line underneath shows the difference between the observed and simulated spectra. Insets show details in certain regions e.g. a magnetic Bragg reflection at very low* q.

structure from a powder diffraction pattern. As a result of a complete refinement, one can show that the low temperature structure of this compound is monoclinic or even triclinic (for solving the metric of the cell, complementary synchrotron x-ray diffraction data is often useful because of the higher achievable q-resolution), i.e. there exists an additional distortion from the Pnma structure introduced in Sec. 12.4. Ferromagnetic order becomes visible by intensity on top of the structural Bragg peak. Antiferromagnetic order is usually (but not always!) connected with an increase in the unit cell dimension, which in turn shows up in the diffractogram by additional superstructure reflections between the main nuclear reflections. It is beyond the scope of this lecture to discuss the experimental and methodological details of such a structure analysis or to present detailed results on specific model compounds. For this we refer to the literature, e.g. [19]. We just want to mention that with detailed structural information, we cannot only determine the lattice- and spin structure, but also the charge- and orbital order and can relate them to macroscopic phenomena such as the CMR effect. At first sight it might be surprising that neutron diffraction is able to give us information about charge order. We have learnt in the introductory chapters that neutrons interact mainly through the strong interaction with the nuclei and through the magnetic dipole interaction with the magnetic induction in the sample. So how can neutrons give information about charge order? Obviously charge order is not determined directly with neutrons. However in a transition metal-oxygen bond, the bond length will depend on the charge of the transition metal ion. The higher the positive charge of the transition metal, the shorter will be the bond to the neighbor-ing oxygen, just due to Coulomb attraction. This qualitative argument can be quantified in the so-called bond-valence sum. There is an empirical correlation between the valence V_i of an ion and the bondlengths R_{ij} to its neighbors:

$$V_i = \sum_{ij} s_{ij} = V_i = \sum_{ij} e^{\frac{R_0 - R_{ij}}{B}}. \tag{12.5}$$

Here, the R_{ij} are the experimentally determined bond lengths, $B = 0.37$ is a constant, and R_0 are tabulated values for the cation-oxygen bonds, see, e.g., [21]. Table 12.1 reproduces some of these values. The sum over the partial "bond-valences" s_{ij} gives the valence state of the ion.

Even though this method to determine the valence state is purely empirical, it is rather precise

Ions	La^{3+}	Pr^{3+}	Nd^{3+}	Sm^{3+}	Eu^{3+}	Gd^{3+}	Tb^{3+}	Dy^{3+}	Er^{3+}
R_0	2.172	2.138	2.105	2.090	2.074	2.058	2.032	2.001	1.988
Ions	Tm^{3+}	Yb^{3+}	Y^{3+}	Ca^{2+}	Sr^{2+}	Ba^{2+}	Mn^{3+}	Mn^{4+}	
R_0	1.978	1.965	2.019	1.967	2.118	2.285	1.760	1.753	

Table 12.1: *R_0 values of cation-oxygen bonds [21] in manganese perovskites needed for the bond valence calculation (12.5).*

compared to other techniques. The values of the valences found with this method differ significantly from a purely ionic model. Instead of integer differences between charges on different transition metal ions, one finds more likely differences of a few tenth of a charge of an electron, though rare exceptions, where near-integer valence differences were observed, exist [22].

Just like charge order, orbital order is not directly accessible to neutron diffraction since orbital order represents an anisotropic charge distribution and neutrons do not directly interact with the charge of the electron. However, we have seen in the discussion of the Jahn-Teller effect (Figs. 12.8 and 12.9) that an orbital order is linked to a distortion of the local environment visible in different bond lengths within the anion complex surrounding the cation. Thus, by a precise determination of the structural parameters from diffraction, one can determine in favorable cases the ordering patterns of all four degrees of freedom: lattice, spin, charge and orbitals.

Is there a more direct way to determine charge- and orbital order? The scattering cross section of x-rays contains the atomic form factors, which are Fourier transforms of the charge density around an atom. Therefore, one might think that charge and orbital order can be easily determined with x-ray scattering. However, as discussed in the last paragraph, usually only a fraction of an elementary charge contributes to charge- or orbital ordering. Consider the Mn atom: the atomic core has the Ar electron configuration, i.e. 18 electrons are in closed shells with spherical charge distributions. For the Mn^{4+} ion, three further electrons are in t_{2g} levels. Since in scattering, we measure intensities, not amplitudes, these 21 electrons contribute $21^2 r_0^2$ to the scattered intensity (the classical electron radius r_0 is the natural unit of x-ray scattering). If the difference in charge between neighboring Mn ions is $0.2\,e$, this will give an additional contribution to the scattered intensity of $0.2^2 r_0^2$. The relative effect of charge ordering in x-ray scattering is therefore only a tiny fraction $\frac{0.2^2}{21^2} \sim 10^{-4}$, even ignoring that scattering from all other atoms makes the situation worse. There is, however, a way to enhance the scattering from non-spherical charge distributions, the so-called anisotropic anomalous x-ray scattering, first applied for orbital order in manganites by Murakami *et al.* [23]. The principle of this technique is depicted in Fig. 12.12, showing scattering from a hypothetical diatomic 2D compound. Non resonant x-ray scattering is sensitive mainly to the spherical charge distribution. A reconstruction of the charge distribution done from such an experiment might look schematically as shown on the left. The corresponding crystal structure can be described with a primitive unit cell (white lines). To enhance the scattering from the non-spherical part of the charge distribution, an experiment can be done at a synchrotron source, with the energy of the x-rays tuned to the energy of an absorption edge (middle). Now, second order perturbation processes can occur, where a photon induces virtual transitions of an electron from a core level to empty states above the Fermi energy and back with re-emission of a photon of the same energy. As second-order per-

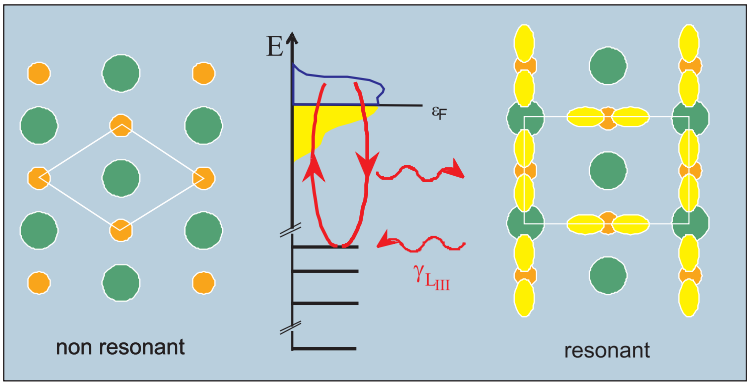

Fig. 12.12: *Anisotropic anomalous x-ray scattering for a hypothetical diatomic 2D compound.* Left*: Reconstruction of the charge distribution from a laboratory x-ray source, sensitive mainly to the spherical charge distribution and corresponding unit cell (white lines).* Middle*: Principles of resonance x-ray scattering in an energy level diagram (see text).* Right*: Charge distribution deduced from such an anomalous x-ray scattering experiment. An orbital ordering pattern is apparent, which could not be detected with non-resonant x-ray scattering. The evidently larger unit cell gives rise to superstructure reflections (at resonance).*

turbation processes have a resonant denominator, this scattering will be strongly enhanced near an absorption edge. If the intermediate states in this resonant scattering process are somehow connected to orbital ordering, scattering from orbital ordering will be enhanced. Thus in the resonant scattering experiment, orbital order can become visible as indicated on the right. With the shown arrangement of orbitals, the true primitive unit cell of this hypothetical compound is obviously larger than the unit cell that was deduced from the non resonant scattering experiment (left), which was not sensitive enough to determine the fine details of the structure. An increase of the unit cell dimensions in real space is connected with a decrease of the distance of the reciprocal lattice points, leading to additional *superstructure reflections*. The intensity of these reflections has the strong energy dependence expected for a second-order perturbation process. This type of experiment is called anisotropic anomalous x-ray scattering, because it is sensitive to the anisotropic charge distribution around an atom.

So far we have discussed some powerful experimental techniques to determine the various ordering phenomena in complex transition metal oxides. Scattering can give much more information than just on the time averaged structure. Quasi-elastic diffuse scattering gives us information on fluctuations and short range correlations persisiting above the transitions, e.g. short range correlations of polarons, magnetic correlations in the paramagnetic state, local dynamic Jahn-Teller distortions etc. Studying these correlations and fluctuations helps to understand what drives the respective phase transitions into long-range order. The relevant interactions, which give rise to these ordering phenomena, can be determined from inelastic scattering experiments as learnt in the chapter on “Inelastic neutron scattering”. For example, in a new class of iron-based high-temperature superconductors, the involvement in Cooper pairing of lattice vibrations or alternatively magnetic fluctuations is controversial, and both of these can be probed in-depth by inelastic neutron scattering (see, e.g., [24]). Since there is a huge amount of scattering experiments on highly correlated transition metal oxides and chalcogenides, a review of these experiments definitely goes far beyond the scope of this introductory lecture.

12.6 Summary

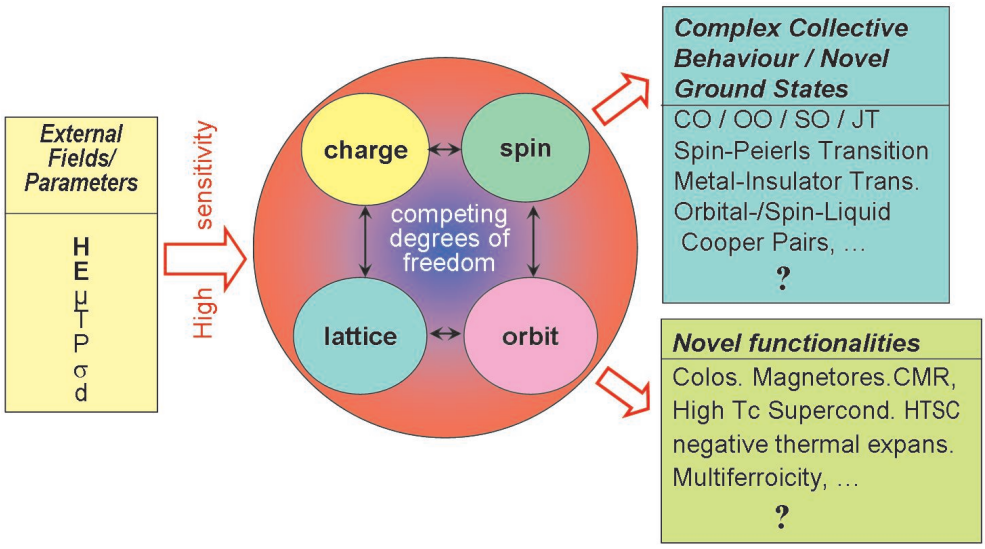

Fig. 12.13: *Illustration of complexity in correlated electron systems.* **H**, **E***: magnetic and electric field, respectively;* μ*: chemical potential (doping);* T*: temperature;* P*: pressure;* σ*: strain (epitaxial growth);* d*: dimensionality (e.g. bulk versus thin film systems); CO: charge order; OO: orbital order; SO: spin order; JT: Jahn-Teller transition.*

This chapter gave a first introduction into the exciting physics of highly correlated electron systems, exemplified by transition metal oxides and chalcogenides. The main message is summarized in Fig. 12.13. The complexity in these correlated electron systems arises from the competing degrees of freedom: charge, lattice, orbit and spin. The ground state is a result of a detailed balance between these different degrees of freedom. This balance can be easily disturbed by external fields or other thermodynamical parameters, giving rise to new ground states or complex collective behavior. Examples are the various ordering phenomena discussed, Cooper pairing in superconductors, so-called spin-Peierls transitions in 1D systems etc. This high sensitivity to external parameters as well as the novel ground states of the systems gives rise to novel functionalities, such as the colossal magnetoresistance effect, high temperature superconductivity, multiferroicity, and many more. A theoretical description of these complex systems starting from first principles, like Schrödinger equation in quantum mechanics or the maximization of entropy in statistical physics, is bound to fail due to the large number of strongly interacting particles. Entirely new approaches have to be found to describe the emergent behavior of these complex systems. Therefore highly correlated electron systems are a truly outstanding challenge in modern condensed matter physics. We have shown in this lecture that neutron and x-ray scattering are indispensable tools to disentangle this complexity experimentally. They are able to determine the various ordering phenomena as well as the fluctuations and excitations corresponding to the relevant degrees of freedom. No other experimental probe can give so much detailed information on a microscopic level as scattering experiments.

Acknowledgement

This lecture bases largely on material from previous lectures given by Th. Brückel.

References

[1] R. B. Laughlin and D. Pines, *Proc. Natl. Acad. Sci. USA* **97**, 28 (2000).

[2] T. Vicsek, *Nature* **418**, 131 (2002).

[3] J. G. Bednorz and K. A. Müller, *Z. Phys. B* **64**, 189 (1986).

[4] A.-M. Haghiri-Gosnet and J.-P., *J. Phys. D: Appl. Phys.* **36**, R127 (2003).

[5] G. Binasch, P. Grünberg, F. Saurenbach, and W. Zinn *Phys. Rev. B* **39**, 4828 (1989).

[6] M. N. Baibich *et al.*, *Phys. Rev. Lett.* **61**, 2472 (1988).

[7] M. H. Phan and S. C. Yu, *J. Magn. Magn. Mater.* **308**, 325 (2007).

[8] E. J. W. Verwey, *Nature* **144**, 327 (1939).

[9] M. Fiebig, *J. Phys. D.: Appl. Phys.* **38**, R123 (2005).

[10] M. Bibes and A. Barthélémy, *Nat.* **7**, 425 (2008).

[11] G. D. Barrera *et al.*, *J. Phys.: Condens. Mat.* **17**, R217 (2005).

[12] E. Dagotto, *Science* **309**, 257 (2005).

[13] N. W. Ashcroft and N. D. Mermin, *Solid State Physics* (Thomson Brooks/Cole, New York, 1976).

[14] H. Ibach and H. Lüth, *Solid State Physics: An introduction to principles of materials science* (Springer, Berlin, 2010).

[15] J. Bardeeen, L. N. Cooper, and J. R. Schrieffer, *Nobel Prize in Physics in 1972 for a microscopic theory of superconductivity (nowadays called BCS-theory.)*

[16] K. Held *et al.*, *J. Phys.: Condens. Mat.* **20**, 064202 (2008).

[17] N. F. Mott, *Rev. Mod. Phys.* **40**, 677 (1968).

[18] P. Fazekas, *Lecture notes on electron correlation and magnetism* (World Scientific, Singapore, 2003).

[19] T. Chatterji (Ed.), *Colossal magnetoresistive manganites* (Kluwer Academic Publishers, Dordrecht, 2004).

[20] A. Urushibara *et al.*, *Phys. Rev. B* **51**, 14103 (1995).

[21] G. H. Rao, K. Bärner, and I. D. Brown, *J. Phys.: Condens. Mat.* **309**, 257 (2005).

[22] M. Angst *et al.*, *Phys. Rev. Lett.* **99**, 086403 (2007).

[23] Y. Murakami *et al.*, *Phys. Rev. Lett.* **81**, 582 (1998).

[24] R. Mittal *et al.*, *Phys. Rev. Lett.* **102**, 217001 (2009).

Exercises

Note: $\star$ indicates an increased difficulty. Solve the easier problems first.

E12.1 Electronic structure and Mott transition

a) In modeling the electronic structure of crystalline solids, what is the typical starting assumption to separate the electronic structure from the lattice dynamics, and why does it work?

b) In which of the three simplest models of electrons in a solid are the electronic correlations taken into account at least approximately?

c) Neglecting electronic correlations, would you predict NaCl to be an insulator or a metal? Why?

d) The competition of which two contributions to the total energy of the electrons is crucial for the Mott-transition? Which further contributions to the total energy are neglected in the simplest model?

e) Assume that a particular material is a Mott-insulator, but just barely so (i.e. the relevant energy contributions are almost equal). What would you predict to happen when sufficiently high pressure is applied, and why?

E12.2 Electronic ordering in correlated-electron materials

a) List and very briefly explain three "electronic degrees of freedom", which can become ordered.

b) $\star$ Discuss why electronic correlations favor ordering processes of these electronic degrees of freedom.

c) What, if any, connection is there between orbital order and orbital magnetic momentum?

d) To order of which of the electronic degrees of freedom is neutron scattering *directly* sensitive, and to which not?

e) For those electronic degrees of freedom, to which neutron is *not* directly sensitive, neutron scattering can still be used to deduce an ordered arrangement: How and why? Is there a more direct scattering method than neutron scattering?

E12.3 Crystal field

Fe has atomic number 26 and in oxides typically has valence states $2+$ or $3+$.

a) Determine the electronic configuration of free Fe^{2+} and Fe^{3+} ions (hint: as for Mn the outermost s-electrons are lost first upon ionization).

b) From Hund's rules determine the values of the spin S, orbital angular momentum L, and total angular momentum J of Fe^{2+} and Fe^{3+} ions.

(*Hund's rules:*

1. S *max.*
2. *L max consistent with 1.*
3. $J = |L - S|$ *for a less than half filled shell,*
   $J = |L + S|$ *for a more than half filled shell*).

c) ⋆ The effective moment μ_{eff} of a magnetic ion can be determined experimentally by the Curie-Weiss law, and is given by $\mu_{\text{eff}} = g_J\sqrt{J(J+1)}\mu_{\text{B}}$, where the Landé factor is

$$g_J = \frac{3}{2} + \frac{S(S+1) - L(L+1)}{2J(J+1)}\,. \tag{12.6}$$

Calculate the expected effective moment in units of μ_{B} of Fe^{2+} and Fe^{3+} ions, i) assuming S, L, and J as determined in b) and ii) setting $L = 0$ ('quenched orbital momentum'). Compare with the experimental values of $\sim 5.88\,\mu_{\text{B}}$ for Fe^{3+} and $\sim 5.25 - 5.53\,\mu_{\text{B}}$ for Fe^{2+}.

d) ⋆ The negatively charged oxygen ions surrounding the Fe ions in an oxide solid influence the energy of the different orbitals. Plot the expected energy level diagram for the case of an octahedral environment of nearest-neighbor O^{2-}. How does the total spin moment of Fe^{2+} change between weak and strong crystal field splittings (relative to intra-atomic "Hund's" exchange)?

e) (optional) ⋆⋆ In a tetrahedral environment the energy levels of the orbitals are reversed compared to an octahedral environment. Determine the spin moment of Fe^{2+} in a tetrahedral environment with strong crystal field splitting. Is an orbital angular momentum possible in this case? How about when a Jahn-Teller-distortion leads to a further splitting of the energy levels?

E12.4 Orbital and Magnetic order in $LaMnO_3$ (Optional!)

The orbital and magnetic order in $LaMnO_3$ is sketched in Fig. 12.9 (page 11 of the chapter) on the left. One crystallographic unit cell $a \times b \times c$ is shown.

a) Why is there no charge order in $LaMnO_3$?

b) What are the smallest unit cells (sketch in relation to the crystallographic cell) that can describe i) magnetic order, ii) ⋆ orbital order (*Hint: consider also centered cells*), iii) both magnetic and orbital order.

c) Make a plot of reciprocal space in the a^*-c^*-plane indicating the positions, where you expect nuclear, orbital, and magnetic Bragg peaks to occur.

d) ⋆ As c), but for the a^*-c^*-plane.